Mem. S.A.It. Suppl. Vol. 1, 145

Memorie della
Supplementi

High-resolution re-simulations of massive DM halos and the Fundamental Plane of galaxy clusters

B. Lanzoni[1], A. Cappi[1], and L. Ciotti[2]

[1] INAF – Osservatorio Astronomico di Bologna, via Ranzani 1, 40127 Bologna, Italy e-mail: lanzoni@bo.astro.it, cappi@bo.astro.it

[2] Dipartimento di Astronomia, Università di Bologna, via Ranzani 1, 40127 Bologna, Italy e-mail: ciotti@bo.astro.it

Abstract. Pure N-body high-resolution re-simulations of 13 massive dark matter halos in a ΛCDM cosmology are presented. The resulting sample is used to investigate the physical origin of the Fundamental Plane, "Faber-Jackson", and "Kormendy" relations observed for nearby galaxy clusters. In particular, we focus on the role of dissipationless hierarchical merging in establishing or modifying these relations. Contrarily to what found in the case of the Faber-Jackson and Kormendy relations for *galaxies* (see Londrillo, Nipoti & Ciotti, this conference), dissipationless merging on *cluster scales* produces scaling relations remarkably similar to the observed ones. This suggests that gas dissipation plays a minor role in the formation of galaxy clusters, and the hierarchical merger scenario is not at odd with the observed regularity of these systems.

Key words. dark matter – galaxies: clusters: general

1. Introduction

Like early-type galaxies, also galaxy clusters follow well defined scaling relations among their main observables: in particular, a luminosity–velocity dispersion relation (i.e., a "Faber-Jackson–like" relation), a luminosity–radius relation (i.e., a "Kormendy–like" relation), and the Fundamental Plane (hereafter FP; e.g., Schaeffer et al. 1993, hereafter S93; Adami et al. 1998; and for ellipticals: Djorgovski et al. 1987; Dressler et al. 1987; Faber & Jackson 1976; Kormendy 1977). Besides their potential importance as distance indicators, these relations contain information on the cluster formation and evolution processes. Within the commonly accepted cosmological scenario, where cold dark matter (CDM) is the dominant component of the Universe, structure formation is driven by hierarchical dissipationless merging: small DM halos form first, then they merge to-

Send offprint requests to: B. Lanzoni
Correspondence to: Osservatorio Astronomico di Bologna,via Ranzani 1, 40127 Bologna

gether to form larger systems, and the evolution of the baryonic matter follows that of the hosting DM halos.

The importance of investigating the physical origin of the observed scaling relations, and the role of dissipationless hierarchical merging in establishing or modifying them, is therefore apparent, and explains the large number of theoretical works devoted to this problem in the case of elliptical galaxies (e.g. Capelato et al. 1995; Nipoti, Londrillo, Ciotti 2002a,b; Gonzales & van Albada 2002; Evstigneeva et al. 2002; Dantas et al. 2002; Londrillo et al., this conference). In particular, it has been shown that, while the FP is reproduced by the end–products of equal mass mergers, the Faber–Jackson and the Kormendy relations are *not* (Nipoti et al. 2002ab; Londrillo et al., this conference). In the case of galaxy clusters however, almost no theoretical studies are devoted to their FP (see, e.g., Pentericci, Ciotti & Renzini 1995; Fujita & Takahara 1999; Beisbart, Valdarnini & Buchert 2001).

We address this problem in the present work, by means of high resolution re-simulations of very massive DM halos (the hosts of galaxy clusters) in a ΛCDM cosmology. Following their hierarchical dissipationless evolution in detail, we verify whether they reproduce the observed scaling relations, both at the present time, and at higher redshift. A full analysis of this work will be given elsewhere (Lanzoni et al., in preparation), while we present here a selection of the main astrophysical results, focusing on the numerical issues.

2. High-resolution re-simulations

To investigate whether the dark matter counterpart of galaxy clusters, as obtained by numerical simulations, do define the observed scaling relations, a large enough sample of very massive DM halos was needed. For this purpose, we have employed the dissipationless "Very Large Simulations" (VLS; see Yoshida, Sheth, & Diaferio 2001), where the simulated comoving volume of the Universe is sufficiently large: the box side is of $479\,h^{-1}$Mpc, with $H_0 = 100\,h^{-1}$ km s^{-1} Mpc^{-1}, and $h = 0.7$. The adopted cosmological model is a ΛCDM Universe with $\Omega_{\rm m} = 0.3$, $\Omega_\Lambda = 0.7$, spectral shape $\Gamma = 0.21$, and normalization to the cluster local abundance, $\sigma_8 = 0.9$. The total number of particles is 512^3, of $6.86 \times 10^{10} M_\odot/h$ mass each.

From these simulations, we have selected a sample of 13 halos with masses between $10^{14} M_\odot/h$ and $2.3 \times 10^{15} M_\odot/h$. They span a variety of shapes, from nearly round to more elongated. The richness of their environment also changes from case to case, with the less isolated halos usually surrounded by pronounced filamentary structures, containing massive neighbors (up to 20% of their mass). All the selected halos are required to have a massive progenitor at redshift $z = 0.5$ (their masses range between 6×10^{13} and $1.5 \times 10^{15} M_\odot/h$), and also at $z = 1$ (with masses between 4×10^{13} and $7 \times 10^{14} M_\odot/h$). Such a choice allows us to study galaxy clusters not only locally, but also at higher redshift.

Given the mass resolution of the simulations, less than 1500 particles compose a halo of $10^{14} M_\odot/h$, and its properties entering the FP relation cannot be accurately determined. We have therefore resimulated at higher resolution the halos in our sample, by means of the technique introduced by Tormen, Bouchet & White (1997), that we briefly summarize in the following.

The first step is to select, in a given cosmological simulation, the halo one wants to reproduce at higher resolution. Then, all the particles composing the selected halo and its immediate surroundings are detected in the initial conditions of the parent simulation: the number of particles within the region thus defined is increased, and the region is therefore called "the high resolution (HR) region". As a consequence, the mean inter-particle separation decreases, and the corresponding high-frequency modes of the primordial fluctuation spectrum are added to those on larger scales originally used in the parent simulation. The overall displacement field is also modified consequently. At the same time, the distribution of surrounding particles is smoothed by means of a spherical grid, whose spacing increases with the distance from the center: in such a way, the original surrounding particles are replaced with a smaller number of *macroparticles*, whose mass grows with the distance from the HR region. Thank to this method, even if the number of particles in the HR region is increased, the total number of particles to be evolved in the simulation remains small enough to require reasonable computational costs, while the tidal field that the overall particle distribution exerts on the HR region remains very close to the original one. For the new initial configuration thus produced, vacuum boundary conditions are adopted, i.e., we assume a vanishing density fluctuation field outside the spherical distribution of particles with diameter equal to the original box size L. A new N-body simulation is then run starting from these new initial conditions, and allows to re-obtain the selected halo at the suited resolution.

We have applied this technique to the 13 massive DM halos selected in the VLS. For 8 out of the 13 selected halos, the resolution has been increased by a factor $\sim$ 33, using high-resolution particles of $\sim 2.07 \times 10^9 M_\odot/h$ each, while a factor of 2 improvement has been adopted for the 5 intermediate mass halos (the particle mass is $10^9 M_\odot/h$ in this case). The gravitational softening used for the high-resolution region is $\epsilon = 5\,\mathrm{kpc}/h$, corresponding to about 0.2% and 0.5% of the virial radius of most and less massive halos, respectively. This scale length represents the spatial resolution of the resimulations, to be compared with that of $30\,\mathrm{kpc}/h$ of the original VLS. Note that to prevent low-resolution macroparticles to "contaminate" the final resimulated halo (i.e., to end within its virial radius), we need to define the HR region not only through the particles of the halo itself in the parent simulation, but considering also a boundary region in its immediate surroundings. This is particularly important in the case of less massive halos, since the small number of their composing particles does not allow to define their encompassing region in the initial conditions with enough precision. To avoid such a "contamination" problem in our re-simulations, a radius of about $3\,r_{\rm vir}$ and $5\,r_{\rm vir}$ for the boundary region was necessary for the most and the less massive halos, respectively. The resulting number of high and low resolution particles are listed in Table 1, together with their sum[1]. To run the resimulations, the parallel dissipationless tree-code "GADGET" (Springel, Yoshida & White 2001) has been used on the IBM SP2 and SP3 of the Centre Informatique National de l'Enseignement Supérieur (CINES, Montpellier, France), and the CRAY T3E of the RZG Computing Center (Munich, Germany), that have comparable processor speed. The number of processors and the CPU time required for the corresponding runs are also listed in Table 1.

Results have been dumped in output files for 100 time steps, equally spaced in the logarithm of the expansion factor of the Universe between $z = 20$ and $z = 0$. At each time step, a Spherical Overdensity (Lacey & Cole 1994) halo finder has been used to detect the halos, and to estimate their virial mass and radius (see Table 1). With respect to the original virial masses and radii, those of the resimulated halos show non-systematic and small differences (of the order of few percent), particularly for the most massive objects. Moreover, also the halo formation history (the way how mass assembly proceeds with time) is very similar to that in the parent simulation, thus assuring the reliability and precision of the high-resolution re-simulation technique we use. Visually, the noticeable improvement provided by such a technique

[1] Note that to get the same mass resolution ($2.07 \times 10^9 M_\odot/h$ or $10^9 M_\odot/h$) in the entire volume of the parent simulation, about 1650^3 of 2100^3 particles of would have been required.

is apparent from Figs. 1 and 2, where the images of the 3 most massive halos, before and after the resimulations, are shown at the scales of $\sim 30\,\mathrm{Mpc}/h$ and $\sim 2\,r_{\rm vir}$, respectively.

3. Observed scaling relations at $z = 0$

Analyzing a sample of 16 nearby galaxy clusters, S93 found the following relation between the observed luminosity and velocity dispersion:

$$L \propto \sigma^{1.87\pm0.44}, \qquad (1)$$

where L is in units of $L_* = 1.325 \times 10^{10}\,h^{-2} L_\odot$ ($h = 1$), and σ in km/s, and between luminosity and radius:

$$L \propto R^{1.34\pm0.17}, \qquad (2)$$

where R is the effective radius measured in Mpc. In both cases, the observed scatter is very large, while a considerable improvement is found when linking the three observables together in a FP-like relation. While a bi-parametric fit was performed by S93, here we derived the FP by means of the Principal Component Analysis (hereafter PCA; see e.g. Murtagh & Heck 1987), that searches for the most suitable combinations of the three observables able to describe a thin plane. By performing a PCA on the data sample of S93, we obtain the new orthogonal variables

$$p_i \equiv \alpha_i \log R + \beta_i \log L + \gamma_i \log \sigma, \qquad (3)$$

with R in Mpc/h, L in $100L_*$, σ in 1000 km/s. In Fig. 3 we show the resulting distribution of the observed clusters (blue triangles) in the (p_1, p_3) and (p_1, p_2) spaces, the former providing an exact edge-on view of the FP and making apparent its small thickness.

4. Scaling relations at $z = 0$ for simulated clusters

To derive the analogous quantities for the simulated clusters, we have constructed their projected radial profiles by counting the DM particles within concentric shells around the center of mass, for three orthogonal directions. Thus, the projected half-mass radius $R_{\rm h}$ has been derived as the radius of the shell containing half the total number of particles, and the velocity dispersion σ has been computed by averaging the squared line of sight component of the (barycentric) velocity over all the particles within $R_{\rm h}$. Since the simulated clusters, as well as the real ones, are not spherical, such a procedure gives different values of $R_{\rm h}$ and σ for the three considered line of sights, the maximum difference never exceeding 33% and 21% in the two cases, respectively. Finally, for converting the DM mass into light, we have adopted a mass–to–light ratio with a small dependence on the luminosity, as suggested by observations (S93; Girardi et al. 2002): $M/L \propto L^\alpha$, with $\alpha = 0.3$. In particular, we have assumed: $M/L = 450(M/M_0)^{\alpha/(\alpha+1)} M_\odot/L_\odot$, where $M_0 = 7.5 \times 10^{14} M_\odot$.

By performing a PCA on the 13 DM halos for the three considered lines of sights, using $R_{\rm h}$, σ, and L computed as just described, we obtain a very well defined and thin FP. To check whether this FP is similar to the observed one, we have also constructed the PCA variables p_i by combining $R_{\rm h}$, σ, and L derived for the DM halos, with the coefficients α_i, β_i, γ_i obtained for the observed clusters. The resulting FP is practically indistinguishable from the observed one, as apparent from Fig. 3. Moreover, also the L-σ and L-R relations of simulated and real clusters are in remarkable agreement (Fig. 4).

Note that assuming a *constant* M/L ratio, the FP of simulated clusters is still well defined, and only shows a mild tilt with respect to the observed one (see solid line in Fig. 3).

5. Scaling relations at higher redshift for simulated clusters

While no observational data are yet available for galaxy clusters at higher redshift,

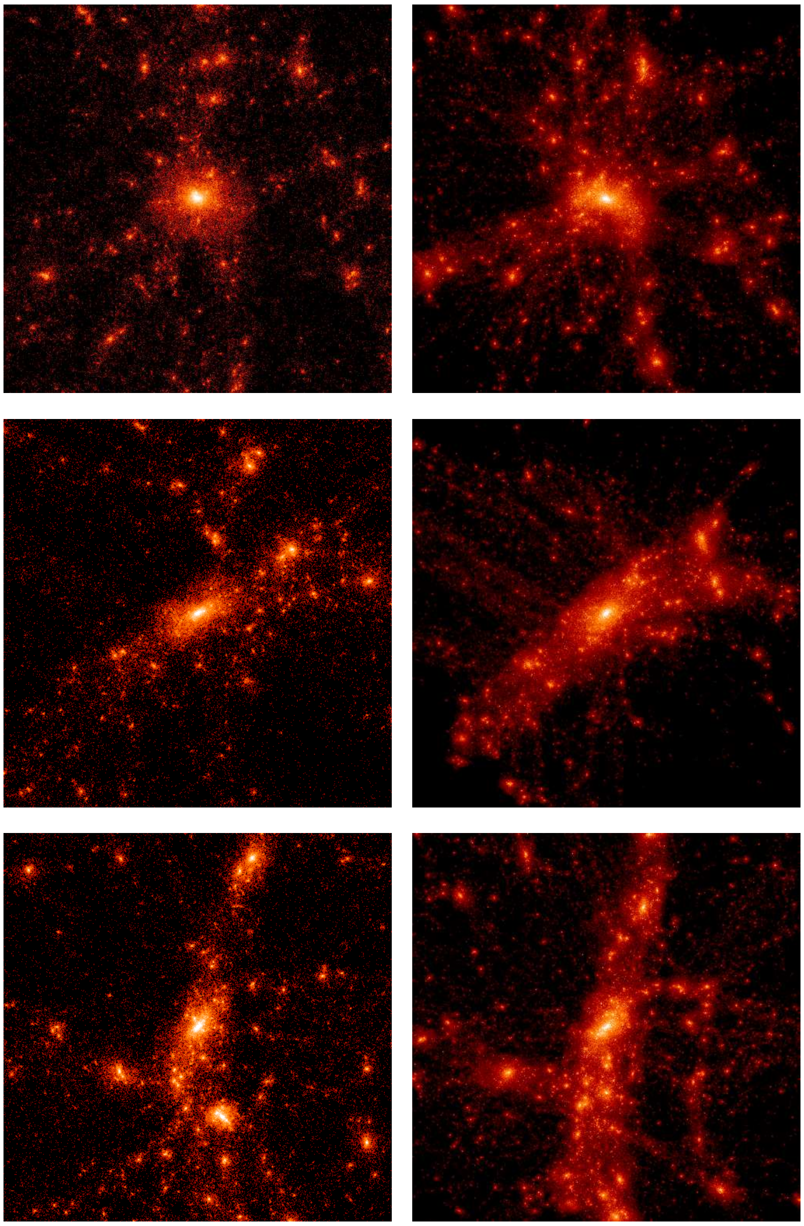

Fig. 1. Images of the 3 most massive DM halos in the parent simulation (left panels) and after the high-resolution re-simulation (right panels). All panels show the projection along an arbitrary line of sight, of a region of $\sim 30\,\mathrm{Mpc}/h$ around the halo center of mass.

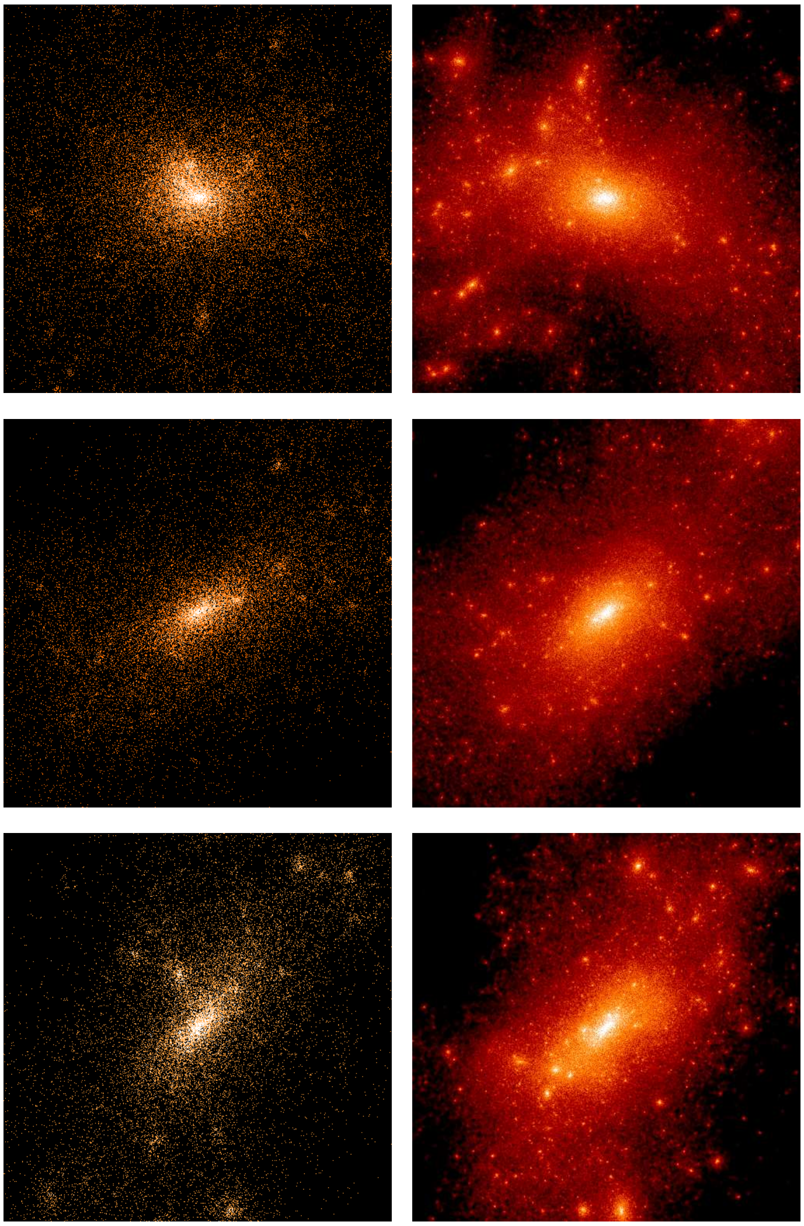

Fig. 2. Images of the 3 most massive DM halos in the parent simulation (left panels) and after the high-resolution re-simulation (right panels). All panels show the projection along an arbitrary line of sight, of a region of $\sim 2\,r_{\rm vir}$ around the halo center of mass.

Table 1. Characteristics of the high-resolution resimulations of the 13 massive halos: N_{HR} = number of high-resolution particles, N_{LR} = number of low-resolution macroparticles, N_T = total number of particles, N_{proc} = number of processors, t_{CPU} = hours per processor required for the resimulations, M_{vir} = virial mass in $10^{14} M_{\odot}/h$, r_{vir} = virial radius in Mpc/h.

Name	N_{HR}	N_{LR}	N_T	N_{proc}	t_{CPU}	M_{vir}	r_{vir}
g8	3700120	191733	3891853	32	80	23.42	2.75
g1	2574717	202301	2777018	32	70	13.99	2.31
g72	3299865	194277	3494142	32	57	11.77	2.18
g696	4870197	184314	5054511	64	60	11.37	2.16
g51	1677364	213477	1890841	32	44	10.78	2.12
g245	3437317	215269	3652586	16	18.4	6.50	1.79
g689	3252085	215809	3467894	16	18.3	6.08	1.75
g564	2068981	227187	2296168	16	12.8	4.91	1.63
g1777	3094123	219047	3313170	16	18.0	3.83	1.50
g4478	2293433	225706	2519139	16	12.8	2.92	1.37
g914	250605	247091	497696	16	7.3	1.45	1.09
g3344	206140	248756	454896	16	6.3	1.09	0.99
g1542	207202	248948	456150	16	6.3	0.82	0.99

our high-resolution re-simulations allow to investigate the scaling relations of their DM counterparts at any epoch. For that purpose, the most massive progenitors at $z = 0.5$ and at $z = 1$ of our 13 DM halos have been considered, and their projected half-mass radius, velocity dispersion and luminosity have been derived with the same procedure used for the $z = 0$ objects. Also in this case, when combining R_h, σ, and L with the coefficients α_i, β_i, γ_i derived for the real clusters at $z = 0$, the resulting FP is very similar to the edge-on FP observed locally, while when seen face-on, the region populated by the high-z DM halos is systematically shifted towards larger (smaller) values of p_1 (p_2) with respect to the region occupied by the observed nearby clusters. In addition, very well defined L-σ and L-R relations are already in place at these redshifts. With respect to the observed L-σ relation at $z = 0$, a flatter slope is found for increasing redshift for the simulated clusters, while the opposite trend is found in the case of the L-R relation, that becomes steeper for increasing z.

6. Discussion and conclusions

We have described a technique for increasing the (mass and spatial) resolution of objects selected in a given cosmological simulation. Applying it to sample of 13 massive halos at $z = 0$ in a ΛCDM cosmology, we have investigated whether the scaling relations observed for nearby galaxy clusters are also followed by their DM hosts, in a dissipationless hierarchical merging scenario. By considering the most massive progenitors at $z = 0.5$ and $z = 1$ of the 13 selected halos, we have also investigated whether the same scaling relations were already in place at those earlier epochs.

The main conclusions can be summarized as follows:

– the high-resolution re-simulation technique is very powerful and reliable. The precision of the method depends on the number of particles composing the original object, and on the dimension of the boundary region considered to avoid the "contamination" from macroparticles.

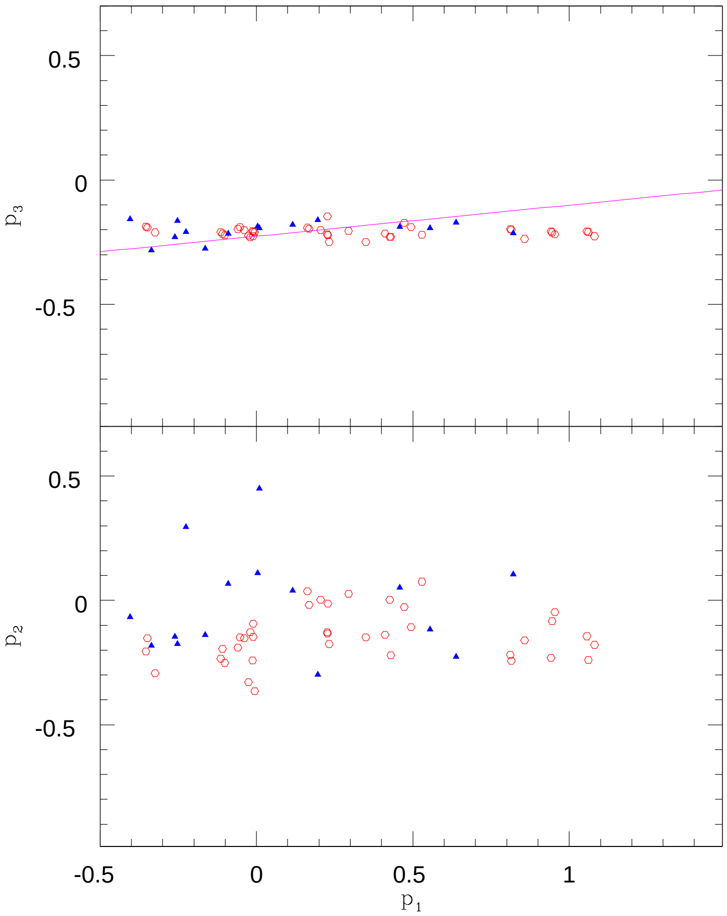

Fig. 3. Observed (blue triangles) and simulated (red hexagons) clusters in the edge-on and face-on view of the FP (upper and lower panels, respectively), at redshift $z = 0$. The linear best fit to the simulated clusters in case of a constant M/L is shown by the pink solid line.

– The DM hosts of galaxy clusters do define a FP that is practically indistinguishable from the one observed for nearby galaxy clusters.
– A very good agreement between the scaling relations of simulated and observed clusters is also found in terms of the L-σ and the L-R relations.
– The FP of simulated clusters is already defined at $z = 0.5$ and $z = 1$, and it is very similar and as thin as the one observed locally; the only differences are due to an obvious shift towards smaller radii and masses for increasing z. Also the L-σ and L-R relations are already in place at high redshifts, with a difference in the slope (with respect to the re-

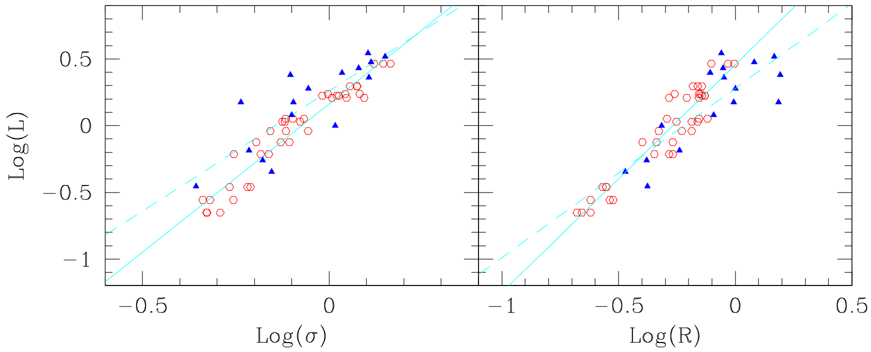

Fig. 4. L-σ (left panels) and L-R (right panels) relations for the observed (blue triangles and dashed line) and simulated (red hexagons and solid line) clusters, at redshift $z = 0$. Luminosities are in units of $100\,L_*$, velocity dispersions in km/s, and radii in Mpc.

lations observed locally) due to the fact that at recent epochs, more massive objects evolve more rapidly than smaller systems.

All the results about the scaling relations of simulated and observed clusters are obtained by assuming a mass-to-light ratio with mean value of the order of $450hM_\odot/L_\odot$ (well in agreement with what estimated from observations of galaxy clusters), and with a dependence on the luminosity also suggested by the observations.

Given the very different nature of the two components (baryonic and non baryonic) and of the physical processes acting on them, the fact that the DM halos define the same relations shown by real clusters is not obvious at all. Moreover, dissipationless hierarchical merging at galactic scales is unable to reproduce the observed scaling relations of elliptical galaxies: the end-products of major mergers do lie on the observed FP, but substantial deviations from the Faber-Jackson and the Kormendy relations are found in this case (see Londrillo et al., this conference). Such a result suggests that, while dissipation has a major role in the formation and evolution of ellipticals, it is negligible with respect to the pure gravity in settling the properties of galaxy clusters.

Acknowledgements. B.L. acknowledges G. Tormen, V. Springel, S. White, & G. Mamon for their help with the N-body simulations and for useful discussions. This work has been partially supported by the Italian Ministery (MIUR) grant COFIN2001 "Clusters and groups of galaxies: the interplay between dark and baryonic matter", and by the Italian Space Agency grants ASI-I-R-105-00 and ASI-I-I-037-01. L.C. was supported by COFIN2000.

References

Adami C., Mazure A., Biviano A., Katgert P., & Rhee G., 1998, A&A 331, 493

Beisbart C., Valdarnini R., & Buchert T., 2001, A&A 379, 412

Capelato H.V., de Carvalho R.R., & Carlberg R.G., 1995, ApJ 451, 525

Dantas C.C., Capelato H.V., Ribeiro A.L.B., & de Carvalho R.R., 2002, MNRAS accepted (astro-ph/0211251)

Djorgovski S., & Davis M. 1987, ApJ, 313, 59

Dressler A., Lynden-Bell D., Burstein D., Davies R.L., Faber S.M., Terlevich R., & Wegner G. 1987, ApJ, 313, 42

Faber S.M., & Jackson R.E. 1976, ApJ, 204, 668
Fujita Y., & Takahara F., 1999, ApJ 519, L55
Evstigneeva E.A., Reshetnikov V.P., Sotnikova N.Ya., 2002, A&A 381, 6
Girardi M., Manzato P., Mezzetti M., Giuricin G., Limboz F., 2002, ApJ 569, 720
Gonzales A.C., & van Albada T.S., 2002, MNRAS submitted
Kormendy J., 1977, ApJ 218, 333
Lacey C., & Cole S., 1994, MNRAS 271, 781
Lanzoni B., Cappi A., Ciotti L., Tormen G., & Zamorani G., in preparation
Murtagh F., Heck A., 1987, *Multivariate Data Analysis*, D.Reidel Publishing Company, Dordrecht, Holland
Nipoti C., Ciotti L., Londrillo P., 2002a, astro-ph/0112133 (NCL02a)
Nipoti C., Ciotti L., Londrillo P., 2002b, MNRAS submitted (NCL02b)
Pentericci L., Ciotti L., & Renzini A. 1995, Astrophysical Letters and Communications, 33, 213
Schaeffer R., Maurogordato S., Cappi A., Bernardeau F., 1993, MNRAS 263, L21 (S93)
Springel V., Yoshida N., & White S.D.M., 2001, New Astronomy, 6, 79
Tormen G., Bouchet F., & White S.D.M., 1997, MNRAS 286, 865
West M.J., Dekel A., Oemler A., 1987, ApJ 316, 1
Yoshida N., Sheth R.K., & Diaferio A., MNRAS 328, 669